SURFACE CHARGING ON ENGINEERING TEST SATELLITE V OF JAPAN

Hironobu NISHIMOTO
Tsukuba Space Center, National Space Development Agency of Japan
2-1-1, Sengen, Tsukuba, Ibaraki 305, Japan

Haruhisa FUJII
Manufacturing Development Laboratory, Mitsubishi Electric Corporation
8-1-1, Tsukaguchi-Honmachi, Amagasaki, Hyogo 661, Japan

Toshio ABE
Kamakura Works, Mitsubishi Electric Corporation
325, Kamimachiya, Kamakura, Kanagawa 247, Japan

ABSTRACT

We developed a potential monitor to measure the surface charging potentials on insulating materials for spacecraft due to charged particles in space environment. The potential monitor was installed on geostationary Engineering Test Satellite V of Japan which was launched on August 27, 1987. Three kinds of thermal control materials were used as samples. We obtained the following observational results: (1)The level of the charging potential depended on the environmental condition and the material. (2)The rapid increase of the charging potential to be due to the shadows of the paddle and/or the antenna was occasionally observed. (3)The potential periodically changed with the temperature inside the sensing part of the potential monitor. (4)For long time, the potential gradually increased under the shaded condition, but decreased in the sunlit condition.

INTRODUCTION

Spacecrafts in Earth orbits have the duties to work normally in tenuous space-plasma environments with solar light and high-energy radiation. The space plasma consists of electrons and positive ions, mainly protons. In high-altitude orbits such as a geostationary orbit, the spacecrafts are considerably affected by these charged particles. The surface potential of a satellite in the space plasma will come into an electrical equilibrium with the potential of the plasma by developing surface charges on the satellite to reduce the net current between the satellite and the plasma to zero (Garrett, 1981; Francis, 1982; Grard et al., 1983). In the situation, the satellite covered with several kinds of insulating materials gets differentially charged. The potential differences between the surfaces of the insulating materials and the electrically conductive surfaces of the satellite could be formed. This phenomenon is reffered to as "differential charging" on the spacecraft (Garrett, 1981; Grard et al., 1983). In particular, when the satellite encounters a hot plasma (or geomagnetic substorm), the potential differences would be multikilovolts. If the potential difference exceeds a breakdown threshold, a discharge will occur (Nanevicz et al., 1980; Purvis et al., 1984).

The differential charging and the discharges on the spacecraft are known to cause the degradation of surface materials, malfunctions and anomalies of on-board electronics, and so on (Garrett, 1981; Francis, 1982; Grard et al., 1983; Purvis et al., 1984). These influences must be minimized to achieve high reliability and long mission of future spacecraft system. So, it is necessary to acquire the charging characteristics of the materials in the actual space environment as well as in ground simulation experiments such as electron-beam irradiation experiments (Stevens et al., 1977; Verdin, 1981; Fujii et al., 1988).

From this viewpoint, we have developed a potential monitor to measure the surface charging potentials of insulating materials for spacecraft due to the charged particles in space (Kawanishi et al., 1986; Nishimoto et al., 1989). The potential monitor which we call as POM was installed on Engineering Test Satellite V (ETS-V) of Japan as one of Technical

Data Acquisition Equipments (TEDA) (Murayama et al.; 1985, Kawanishi et al., 1986). ETS-V is the first domestically developed 3-axis stabilized geostationary satellite in Japan. It was launched from Tanegashima Space Center on August 27, 1987 and settled at 150 degrees of east longitude on the geostationary orbit.

This report describes the outline of the POM briefly and the electrostatic charging characteristics of the insulating materials which have been obtained by the POM on ETS-V for about two years (Nishimoto et al., 1989).

OUTLINE OF POTENTIAL MONITOR (POM)

The POM has the function to measure the surface charging potentials on typical insulating materials for spacecraft in the geostationary orbit and has the objective to study the electrostatic charging and discharging phenomena in cooperation with Discharge Monitor (DIM) which is also one of the TEDA (Kawanishi et al., 1986). It is expected that the acquired data are served to protect future spacecrafts from the influences caused by the electrostatic charging and discharging.

The block diagram of the POM is shown in Fig.1. The POM consists of sensing part (POM-S) and electronics (POM-E). The POM-S to be exposed to space environment is connected by cables to the POM-E. Electrostatic probe (Monroe Inc., 1017S) is located in the POM-S. The probe has an electrostatic electrode, a high-impedance pre-amplifier, a microfork chopper and the driver. The POM-E consists of two amplifiers, a phase-sensitive demodulator and an oscillator.

The sample board is set on the POM-S. A sample with metallized backing is pasted on the sample board with a conductive adhesive (ECCOBOND 56C). However, a non-metallized region of diameter of 1mm is formed on the back of the sample. The electric field which the accumulated charges generate on the front surface is detected through the non-metallized region by the electrostatic probe and the signal is recorded as the output voltage of the POM-E.

The relation between the front surface potential and the output voltage of the POM-E was calibrated by applying a known potential to a metallic plate put on the front surface. And it was also calibrated by measuring the surface potential with the electrostatic voltmeter as irradiating the front surface with an electron beam with energy of 15keV. The measurement range of the surface potential is +1kV to -10kV.

The external dimension and the photograph of the POM-S (flight model) are shown in Fig.2 and Fig.3, respectively. The POM-S consists of three sensing parts. Each sensing part has one sample of insulating material whose size is 40x40mm^2. The test samples installed on the POM-S are as follows;

1)Aluminized Kapton of 127μm thickness,
2)Silvered fused-silicate-glass of 200μm thickness (OSR: Optical Solar Reflector),
3)Silvered Teflon (FEP; fluorinated ethylene propylene copolymer) of 127μm thickness.

The POM-S is set on the south mission panel of ETS-V whose external appearance is shown in Fig.4. The POM-S is connected by cables to the POM-E which is located in the body of ETS-V in order to protect the electronics from high-energy radiation.

The POM was switched on by a command on September 7, 1987.

OBSERVATIONAL RESULTS

The following charging characteristics of the insulating materials in the space environment have been obtained for about two years.

Figure 5 shows the charging potentials on October 28, 1987. Until October 28, the amplitude of the surface potentials of the three materials was

OSR ≧ Kapton > Teflon,

and the potential of the OSR was beyond -10kV, the upper limit of the measurable potential. At 8:00 UT (Universal Time) on October 28, the rapid decrease of the surface potential of the OSR was observed. After that, the OSR was positively charged and the amplitude of the surface potentials of the three materials was

Kapton > Teflon > OSR.

After a few months, the surface potential of the Kapton sample became beyond −10kV.

Figures 6 and 7 show the surface charging potential of the Teflon sample with the count rates of high-energy electrons and protons on October 26 and 27, 1987, respectively. We referred to the data of the count rates of electrons (>2MeV) and protons (1.4 − 4MeV) measured by Space Environment Monitor (SEM) equipped on Geometeorological Satellite 3 (GMS-3) of Japan, "Himawari-3", which is on the geostationary orbit of 140 degrees of east longitude. The surface potentials negatively increased about 14:00UT to 20:00UT. The similar increase of the surface potentials can be also seen in Fig.5. The amplitude of the potential increase on October 27 was larger than that on October 26. October 27 was the more disturbed day than October 26, which is indicated from the count rates of the electrons and protons in Fig.6 and Fig.7.

We also observed that the surface potentials of the Teflon sample slightly changed with the temperature inside the POM-S as shown in Fig.8 (Nishimoto et al., 1989). However, there is a time lag between the charging potential and the temperature.

Figure 9 (a) and (b) show the surface potential of the Teflon sample which have been measured for about two years. In these figures, the surface potentials at 0:00UT of every day were recorded. The potential gradually increased with time from February to September, 1988 (Fig.9 (a)). It decreased from October, 1988 to February, 1989. After that it also changed to tend to increase from February to September, 1989 (Fig.9 (b)).

DISCUSSION

In general, the formation of the surface potential V_s on an insulating material in a charged-particles environment is expressed as follows (Garrett, 1981; Purvis et al., 1984);

$$dV_s/dt = A/C \cdot (J_e - (J_p + J_{se} + J_{bs} + J_{ph} + J_c)), \quad \cdots\cdots (1)$$

where

J_e; incident electron current density,
J_p; incident positive-ion current density,
J_{se}; secondary electron current density,
J_{bs}; back-scattered electron current density,
J_{ph}; photo-emitted electron current density,
J_c; conduction current density through the bulk of the material,
A; exposed area of the material,
C; capacitance of the material,
t; time.

Taking this equation (1) into account, we will discuss the observational results.

Since the POM-S was set on the south mission panel of ETS-V, the POM-S is in the sunlit condition from the autumnal equinox (September 23) to the vernal equinox (March 20). The rest of a year gives the shaded condition to the south mission panel. The incident angle of solar light to the south mission panel changes with time in the sunlit condition. As ETS-V has the structure shown in Fig.4, the shadows of the L-band antenna reflector and/or the solar array paddle are considered to be cast on the south mission panel depending on the position of the orbit. As an example, the shadows which are formed on the south mission panel at 1:40 LT (Local Time) on a certain day near the winter solstice are shown in Fig.10. The shadow is cast on the POM-S at least three times during 0:00LT and 12:00LT. (0:00 LT corresponds to 14:00 UT.)

When the shadow is cast on the insulating material, the effect of photo-electron emission from the surface disappears. In the equation (1), J_{ph} becomes zero and the surface potential V_s negatively increases. The rapid increases of the surface potentials about 14:00UT to 20:00UT as shown in Fig.5, Fig.6 and Fig.7 are considered to be due to the shadow formed on the POM-S. As the shadow is formed on the POM-S about the same time every day, the increase of the surface potentials should have been observed every day. However, the increase is not always observed every day as shown in Fig.8. The observed charging properties are not explained only by the effect of the shadow. At this stage, however, the reason is not clear.

From the comparison between the SEM data of GMS-3 in Fig.6 and that in Fig.7, the conditions of the charged particles on October 27 is considered to have been more disturbed than that on October 26. Under the disturbed condition, the fluxes and the average energies of the charged particles increase (for example, Purvis et al., 1984). In this case, the incident electron current density to the satellite surface, J_e in the equation (1), increases. Also, as seen in the SEM data in Fig.7, the count rate of the proton drastically decreased on October 27. This may cause the decrease of the incident proton current density J_p. From these, the amplitude of the surface potential change in the shadow becomes large as seen in Fig.7.

Figure 8 shows that the surface potential of the Teflon sample periodically changed with the temperature inside the POM-S. To clarify whether the periodical change of the surface potential is due to the electronic circuit used in the POM-S or due to the sample material itself, we tested the temperature dependence of the electronic circuit. The test was performed by applying a constant voltage to a metallic plate on the POM-S and changing the ambient temperature from -20°C to 40°C. Figure 11 shows the result. This indicates that the output voltage has no temperature dependence. Therefore, we concluded that the periodical change of the surface potential is affected by the temperature dependence of the sample material itself.

Generally, the volume resistivity ρ of an insulating material decreases with the temperature as follows (for example, O'Dwyer, 1973);

$$\rho = \rho_0 \cdot \exp(E_a/kT), \quad \cdots (2)$$

where E_a, k and T are the activation energy of the insulating material, Boltzmann' constant and the absolute temperature, respectively. ρ_0 is a constant value for the material. ρ_0 and E_a are determined by experiments. Then J_i (leakage current density through the bulk of the material) increases with increase of the temperature. Therefore, from the equation (1), the charging potential decreases with the temperature.

In Teflon (FEP), E_a is reported as 1.95eV (for example, Gross, 1980) and the volume resistivity ρ at room temperature (300K) is 2×10^{18} Ω cm. We calculated the temperature dependence of the surface potential of the Teflon (FEP) sample installed on ETS-V by using these values, the equivalent electrical circuit model as shown in Fig.12 (Massaro et al., 1977) and the environmental condition measured by SCATHA satellite (Mullen and Gussenhoven, 1982; Purvis et al., 1984). The result is shown in Fig.13. This indicates that the decrease of the volume resistivity ρ of Teflon due to the temperature increase decreases the surface potential. Therefore, the periodical change of the temperature inside the POM-S whose period is one day causes that of the surface potential of the Teflon sample.

And the fact that the sample is exposed to the space environment and the temperature sensor is inside the POM-S causes the time lag between the surface potential and the temperature.

If the same charge density is deposited on the front surface of each sample, the amplitude of the potentials ought to be

Teflon > OSR > Kapton,

when taking the thickness and the dielectric constant into consideration. (The dielectric constants of Teflon, OSR and Kapton are 2.1, 3.9 and 3.5 respectively.) In fact, it is reported that the amplitude of the charging potentials was

Teflon > OSR > Kapton

in shadow by Satellite Surface Potential Monitor on SCATHA satellite on April 29, 1979 (Mizera, 1981).

However, our observational result indicated that the potential of the Teflon sample is lower than that of the Kapton as shown in Fig.5. This may be due to the difference of the secondary-electron emission properties. The rapid decrease of the surface potential of the OSR was observed at 8:00UT on October 28, 1987 as shown in Fig.5. This may indicate that the surface discharge occurred on the OSR. (However, the Discharge Monitor did not detect the signal in the event.) According to our ground simulation experiment, OSR is, however, vulnerable to discharge at the edge (Fujii et al., 1988).

As shown in Fig.9, the surface potential of the Teflon sample at 0:00 UT had a gradual change for long term of two years. In the sunlit condition, the surface potential gradually decreased. On the other hand, in the shaded condition, it gradually increased. From these data, we calculated the rates of the change of the deposited charges, dQ/dt. The results are shown in Fig.9. We estimate the results as follows. High-energy electrons penetrate deeply in the bulk of the sample. These are gradually accumulated in the bulk of the sample under the shaded condition, irrespective of the leakage of electrons through the bulk. However, these electrons are gradually photo-emitted with weak intensity of the solar light due to large incident angle of solar light because the POM-S is set on the south mission panel of ETS-V as described previously.

As shown in Fig.9, dQ/dt from February to September of 1989 is smaller than that from February to September of 1988. It is considered that the Teflon sample was deteriorated by high-energy radiation for long time and the volume resistivity decreased.

CONCLUDING REMARKS

The following results of the surface charging on the insulating materials were obtained by the POM installed on ETS-V.

(1)The level of the charging potential depended on the environmental condition and the material.

(2)The rapid increase of the potentials was occasionally observed. It seems to be due to the shadows of the antenna and/or the solar array paddle.

(3)The potentials periodically changed with the temperature inside the POM-S.

(4)For long time, the potentials gradually increased under the shaded condition, but decreased in the sunlit condition.

The data on the surface potentials are normally obtained by the POM on ETS-V until now.

We are now developing an improved POM for ETS-VI (to be launched in 1993) from the experience of the development and the performance of the POM installed on ETS-V.

REFERENCES

Francis, C.R.;"Electrostatic charging problems of spacecraft," J. Electrostatics, vol.11 (1982) p.265

Fujii, H., Y.Shibuya, T.Abe, R.Kasai and H.Nishimoto;"Electrostatic charging and arc discharges on satellite dielectrics simulated by electron beams," J. Spacecraft & Rockets, vol.25 (1988) p.156

Garrett, H.B.;"The charging of spacecraft surfaces," Rev. Geophys. Space Phys., vol.19 (1981) p.577

Grard, R., K.Knott and A.Pedersen;"Spacecraft charging effects," Space Science Rev., vol.34 (1983) p.289

Gross, B.;"Radiation-induced charge storage and polarization effect," "Electrets" edited by G.M.Sessler (Springer Verlag, Berlin) (1980) p.217

Kawanishi, T., H.Nishimoto, T.Koizumi and T.Abe;"Satellite Environmental Monitor and Material Degradation Monitor installed on Engineering Test Satellite (ETS-V)," IFAC Workshop on Electrostatic Charges and Discharges and Cosmic Ray Interaction in Satellites (1986)

Massaro, M.J., T.Green and D.Ling;"A charging model for three-axis stabilized spacecraft," Proc. Spacecraft Charging Technology Conf., AFGL-TR-77-0051/NASA-TMX-73537 (1977) p.237 **ADA045459**

Mizera, P.F.;"Charging results from the Satellite Surface Potential Monitor," J. Spacecraft & Rockets, vol.18 (1981) p.506

Mullen, E.G. and M.G.Gussenhoven;"SCATHA environmental atlas," AFGL-TR-83-0002 (1983) **ADA131456**

Murayama, H., K.Nakamaru, S.Yamada, T.Ueda, R.Kasai and M.Ohmura;"Experiments by ETS-V," J. Space Technology and Science, vol.1 (1985) p.20

Nanevicz, J.E. and R.C.Adamo;"Occurrence of arcing and its effects on space systems," Prog.

Astron. Aeron., vol.71 (1980) p.252
Nishimoto, H., H.Fujii and T.Abe;"Observation of surface charging on Engineering Test Satellite V of Japan," AIAA 27th Aerospace Science Meeting, AIAA-89-0613 (1989)
O'Dwyer, J.J.;"The theory of electrical conduction and breakdown in solid dielectrics" (Clarendon Press, Oxford) (1973)
Purvis, C.K., H.B.Garrett, A.G.Whittlesey and N.J.Stevens;"Design guidelines for assessing and controlling spacecraft charging effects," NASA Technical Paper 2361, (1984)
Stevens, N.J., F.D.Berkopec, J.D.Staskus, R.A.Blech and S.J.Narciso;"Testing of typical spacecraft materials in a simulated substorm environment," Proc. Spacecraft Charging Technology Conf., AFGL-TR-77-0051/NASA-TMX-73537 (1977) p.431 **ADA045459**
Verdin, D.;"Electrostatic charging of spacecraft materials," J. Electrostatics, vol.11 (1981) p.249

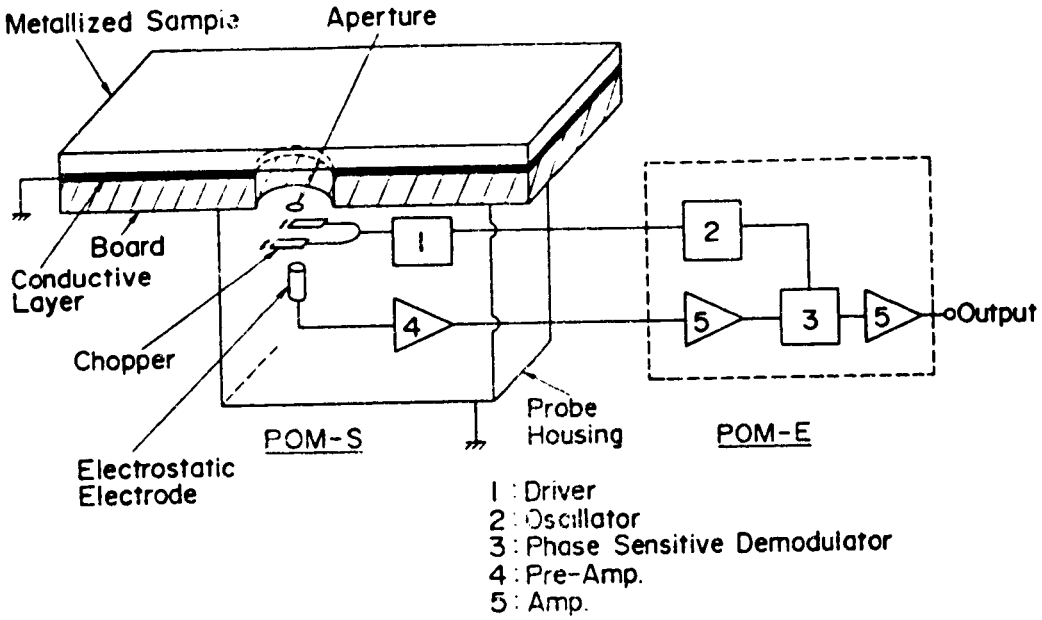

Fig.1 Block diagram of POM.

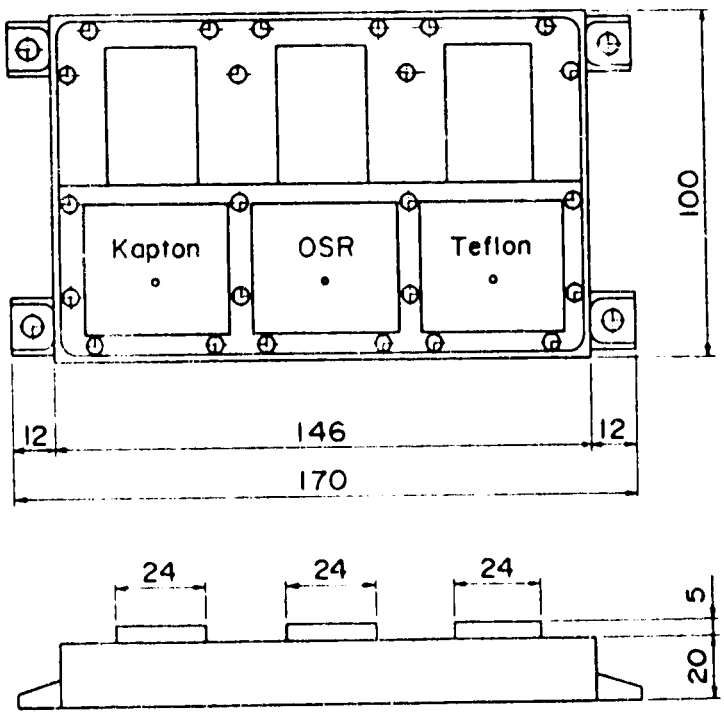

Fig.2 External dimension of POM-S installed on ETS-V.

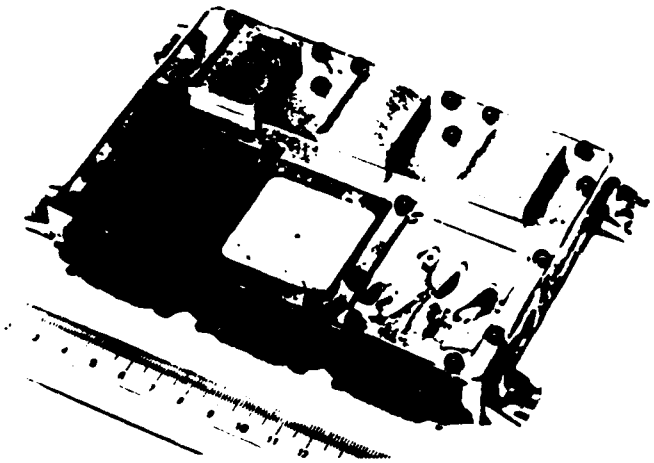

Fig.3 Photograph of POM-S installed on ETS-V.

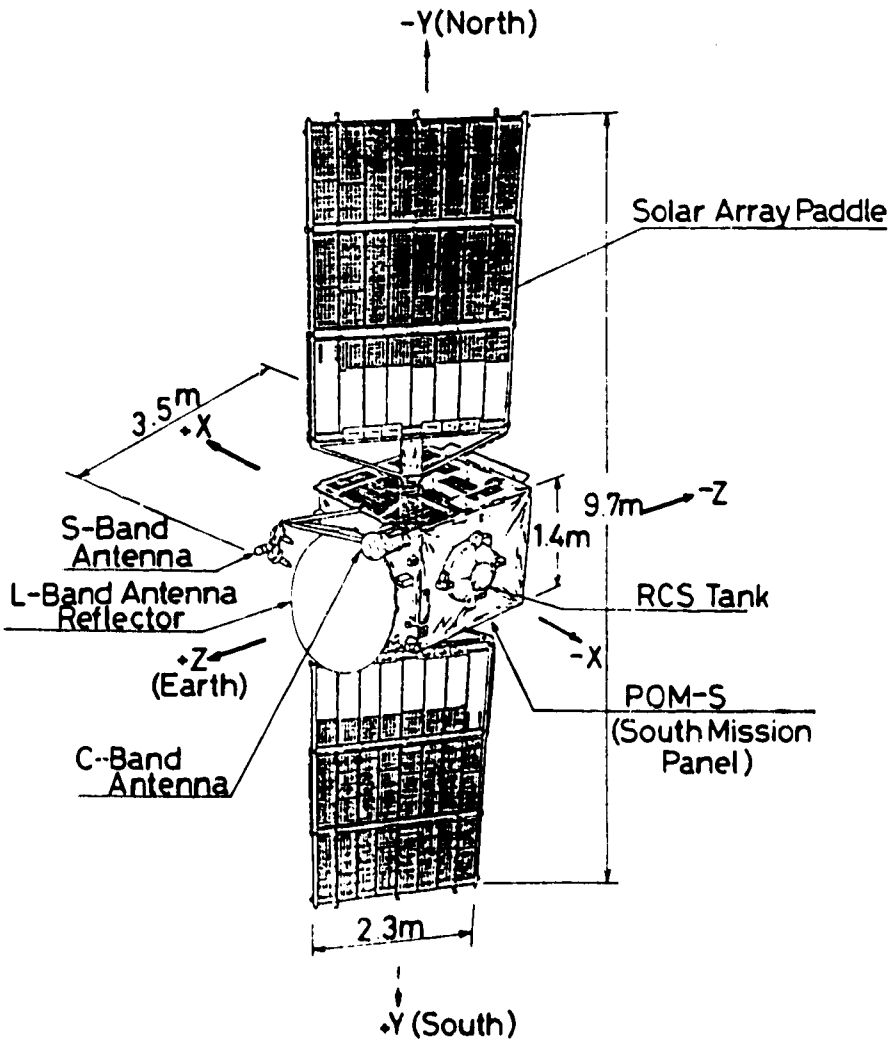

Fig.4 External appearance of ETS-V.

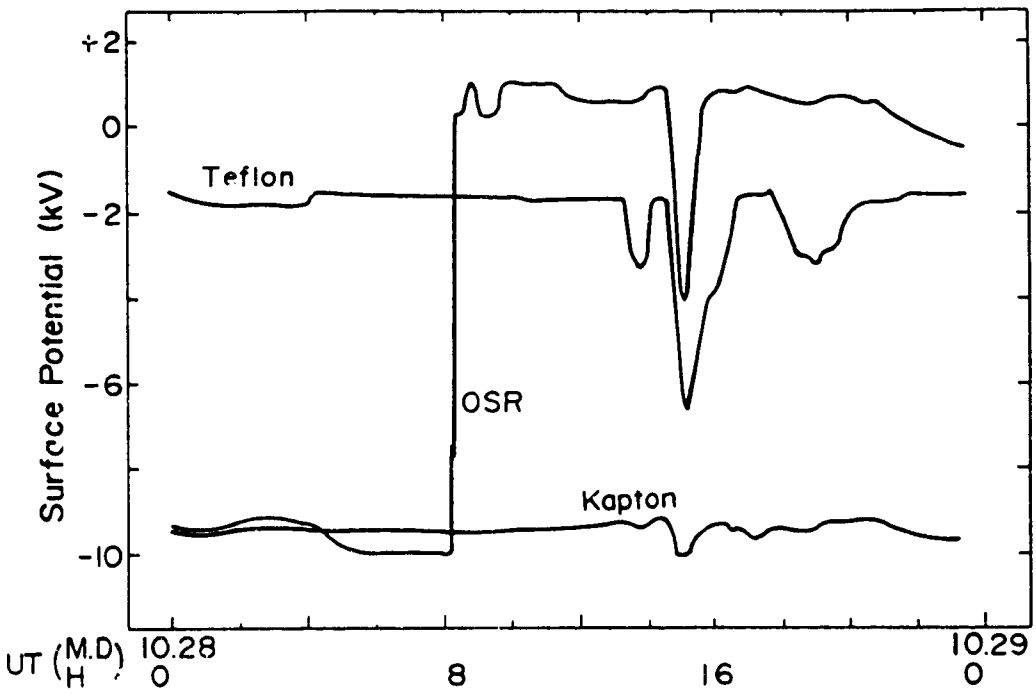

Fig.5 Surface charging potentials on October 28, 1987.

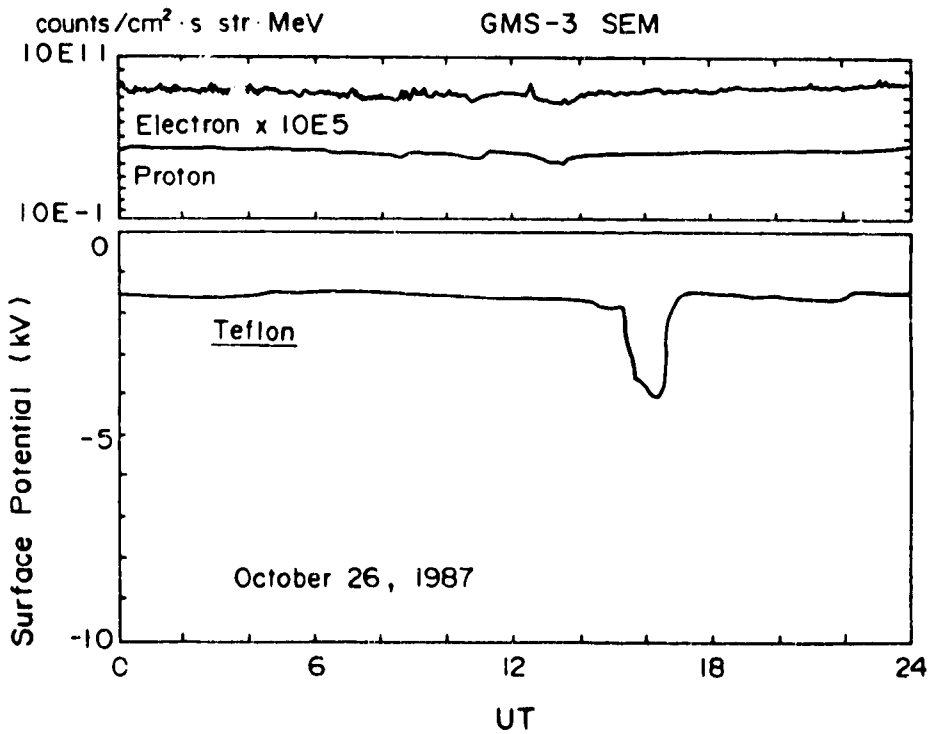

Fig.6 Surface charging potential of Teflon and count rates of electrons (>2MeV) and protons (1.4 - 4MeV) on October 26, 1987.

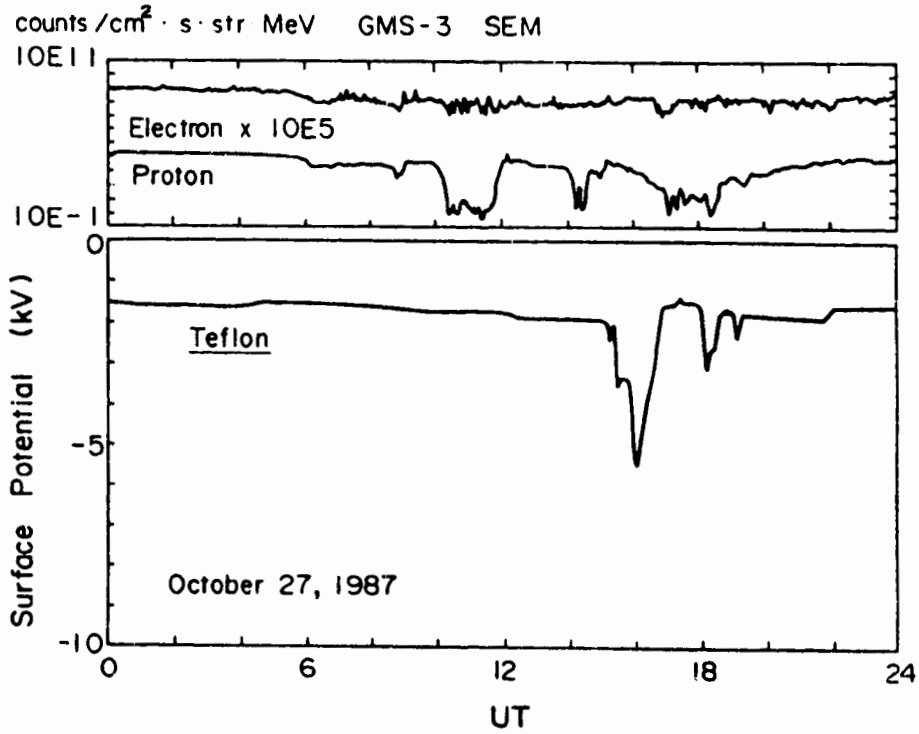

Fig.7 Surface charging potential of Teflon and count rates of electrons (>2MeV) and protons (1.4 – 4MeV) on October 27, 1987.

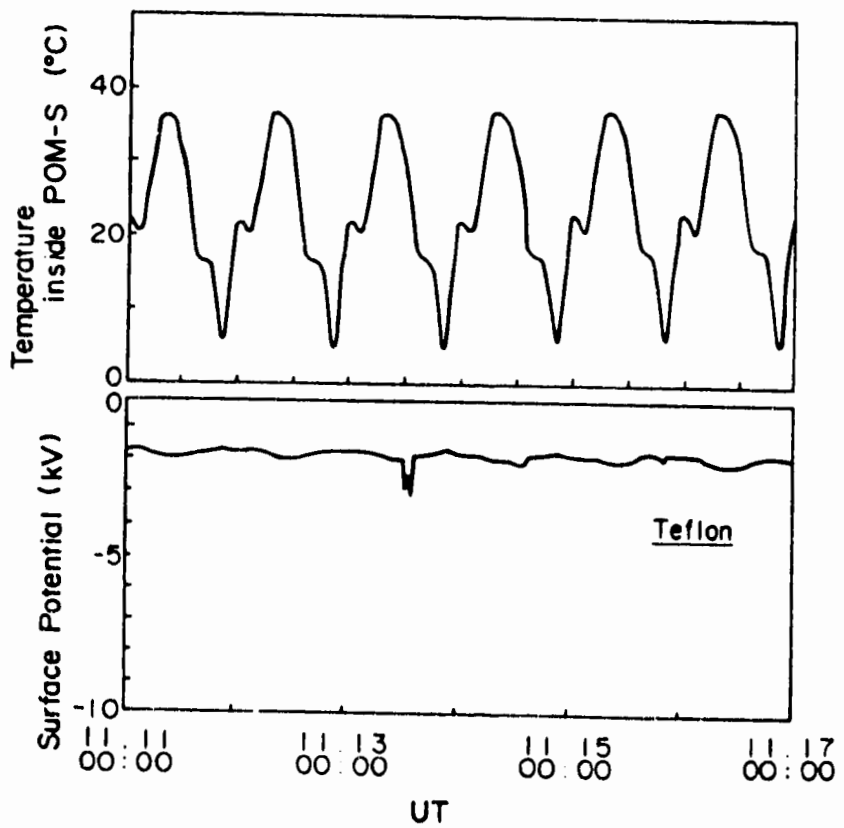

Fig.8 Surface charging potential of Teflon and temperature inside the POM-S on November 11 to 16, 1987.

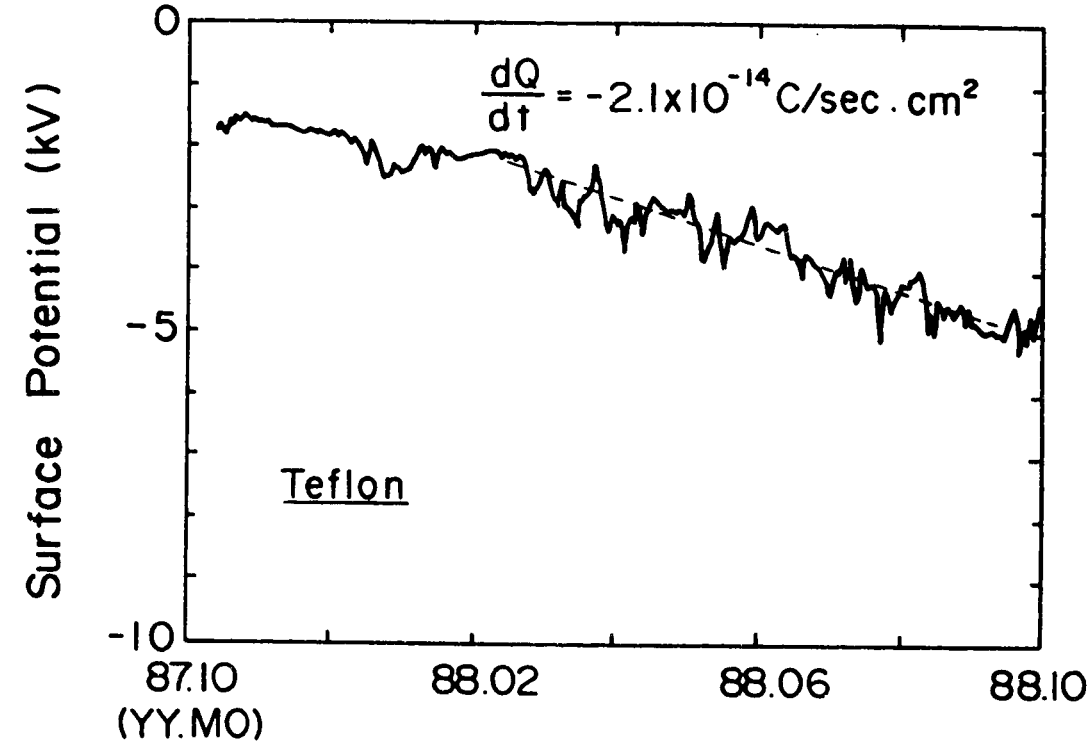

(a)

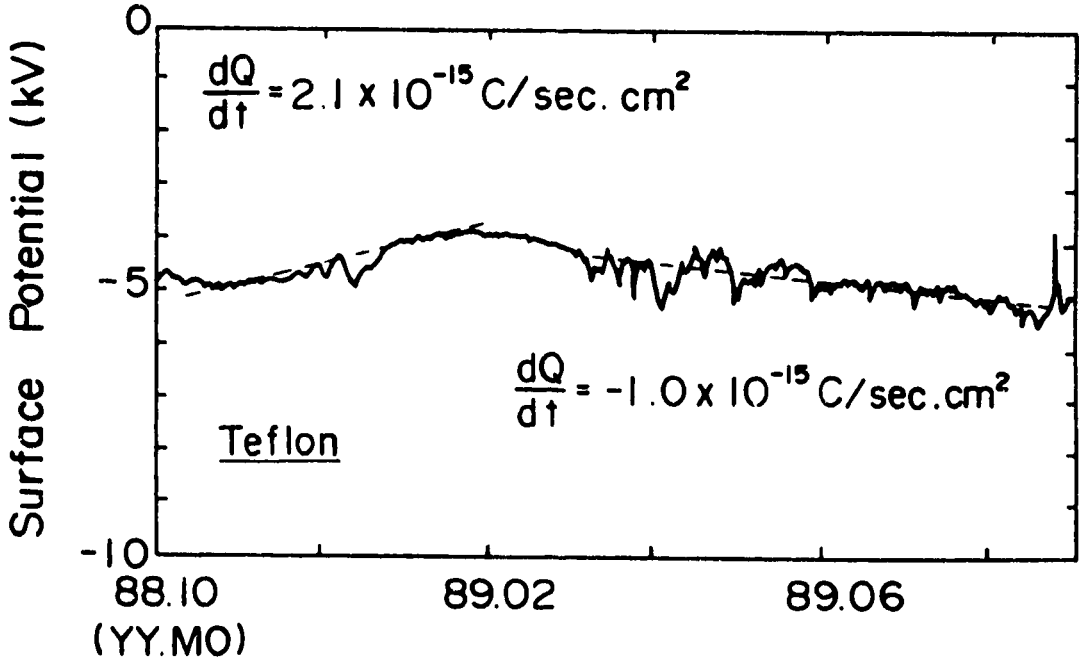

(b)

Fig.9 Surface charging potential of Teflon at 0:00UT from October, 1987 to September, 1989.

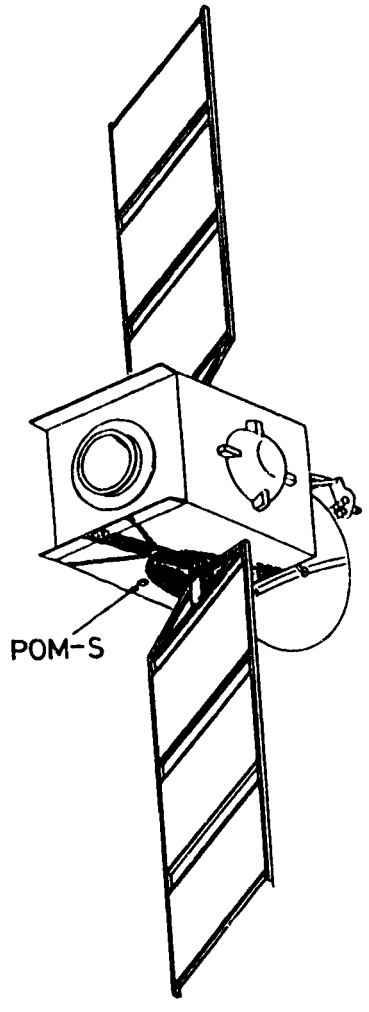

Fig.10 Shadows cast on the south mission panel of ETS-V at 1:40LT on one day near the winter solstice.

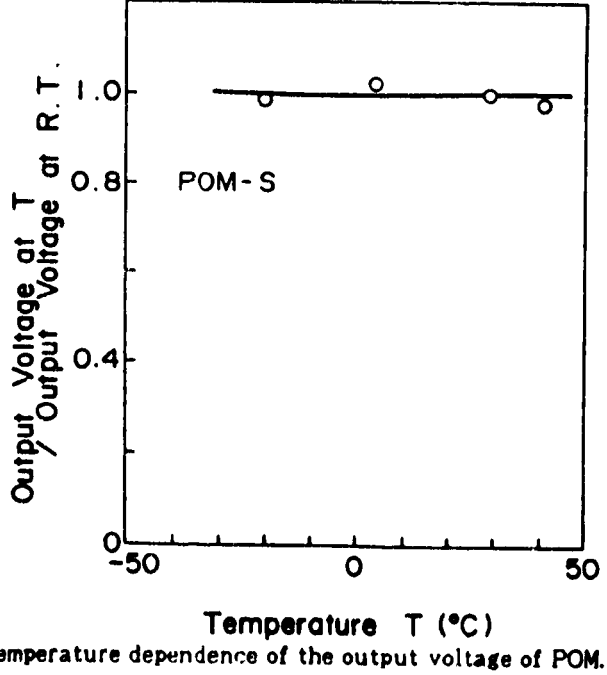

Fig.11 Temperature dependence of the output voltage of POM.

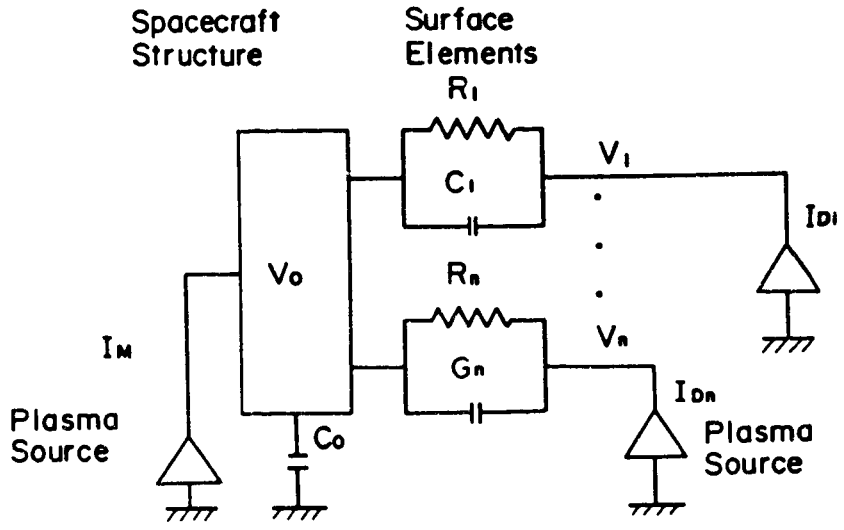

Fig.12 Spacecraft equivalent circuit model (Massaro et al., 1977).

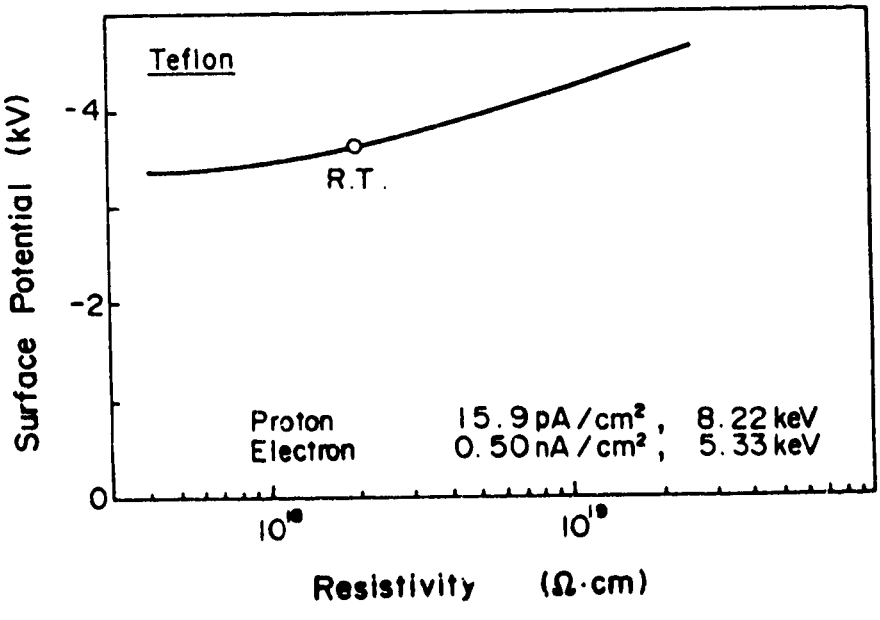

Fig.13 Surface potential of Teflon calculated by using the model shown in Fig.12.